Electron energy-loss near-edge structures at the oxygen K edges of titanium(IV) oxygen compounds

1992 J. Phys.: Condens. Matter 4 3429

(http://iopscience.iop.org/0953-8984/4/13/007)

J. Phys.: Condens. Matter 4 (1992) 3429–3437. Printed in the UK

Electron energy-loss near-edge structures at the oxygen K edges of titanium(IV) oxygen compounds

R Brydson†|| H Sauer‡, W Engel‡ and F Hofer§

† The Blackett Laboratory, Imperial College, Prince Consort Road, London SW7 2BZ, UK

‡ Fritz-Haber-Institut der Max-Planck-Gesellschaft, Faradayweg 4-6, W-1000 Berlin, Federal Republic of Germany

§ Forschungsinstitut fur Elektronenmikroskopie und Feinstrukturforschung, Technische Universitat Graz, Steyrergasse 17, A-8010 Graz, Austria

Received 13 August 1991, in final form 9 January 1992

Abstract. Electron energy-loss near-edge structures at the oxygen K edges of a number of titanium(IV)–oxygen compounds have been measured with an energy resolution of 0.5 eV. A detailed interpretation of the observed structures in terms of the differing nearest-neighbour coordinations of oxygen is obtained by comparing the experimental spectra with the results of multiple-scattering calculations and some theoretical densities of states derived from the literature.

1. Introduction

Electron energy-loss spectroscopy (EELS) conducted in a transmission electron microscope constitutes an important probe of the solid state. Ideally suited to the measurement of the core loss edges of light elements, analysis of the electron energy-loss near-edge structure (ELNES) associated with each edge provides an insight into the local electronic and geometrical structure [1–4].

We have already published a detailed EELS study of the titanium dioxide polymorphs rutile and anatase [5] and in this work we consider the oxygen K edges of further titanium(IV)–oxygen compounds in order to correlate the differences in the environments of the oxygen atoms with the observed differences in the O K ELNES. This seemed to be of particular importance because the lowest unoccupied bands in all these compounds are known to have the same origin and a similar structure.

Considering the dipole selection rule appropriate to EELS measurements made with a small collection semi-angle, the oxygen K edge essentially involves transitions from the oxygen 1s core level to unoccupied final states of p character centred on the oxygen atom. In the single electron picture the observed O K ELNES therefore simply reflects the oxygen p projected unoccupied density of states (DOS); however, in reality the final state DOS may be modified by electron–core hole interaction as well as correlation interactions. De Groot *et al* [6] argue that, for the O K edges of transition-metal oxides, these effects should be small because, while the core hole is situated on the oxygen atom, the unoccupied states just above the Fermi level

|| Present address: Department of Materials, University of Oxford, Parks Road, Oxford OX1 3PH, UK.

0953-8984/92/133429+09$04.50

are of principally metal 3d character and therefore have most weight on the metal sites. Hybridization between oxygen 2p levels and the unoccupied metal d bands does occur; however, the core hole should only influence the final-state DOS indirectly. Furthermore, the core hole will be to some extent screened by the predominantly O 2p valence band electrons.

2. Materials and methods

2.1. Crystal structures

The Ti(IV) oxides studied include $SrTiO_3$ and $BaTiO_3$ both of which possess the cubic perovskite structure [7, 8]. The nearest-neighbour environment of oxygen in this structure consists of two Ti atoms arranged in a linear Ti–O–Ti unit (the site symmetry of oxygen is D_{4h}). Also included are the three polymorphs of TiO_2: rutile, anatase and brookite; rutile and anatase are both tetragonal while brookite is orthorhombic [7]. In all three, however, oxygen is coordinated to three titanium atoms. In rutile and anatase this coordination is such that all atoms lie in a planar unit (oxygen site symmetry, C_{2v}) whereas brookite possesses two inequivalent oxygen sites which are both slightly distorted from the plane (oxygen site symmetry, C_1). In terms of bond angles, one oxygen site in brookite resembles that in anatase while the other is more like that found in rutile. A further titanium(IV) oxide is ilmenite ($FeTiO_3$) which possesses a rhombohedral structure [7]. Here oxygen is coordinated to four atoms—two titanium and two iron atoms—with considerable distortions from perfect tetrahedral symmetry (oxygen site symmetry, C_1). Finally we include the mineral titanite ($CaTiSiO_5$), which contains three distinct oxygen sites which are chemically (i.e. they possess differing nearest-neighbour species) as well as structurally inequivalent [7]. One oxygen site, O(1), is coordinated to two titanium atoms and one calcium atom (oxygen site symmetry, C_2) within a cage of oxygen atoms at about 5 au. Another, O(2), is coordinated to one silicon, one titanium and two calcium atoms (oxygen site symmetry, C_1) within a similar oxygen cage. The third, O(3), is coordinated to one silicon, one titanium and one calcium atom (oxygen site symmetry, C_1) together with the close approach of an oxygen atom (O(3)) within the surrounding oxygen cage at 5 au. The relative occupancies O(1):O(2):O(3), of the three oxygen sites, are 1:2:2.

2.2. Instrumentation and experiment

The instrument used for the EELS measurements has been described elsewhere [9]; briefly it consists of a scanning transmission electron microscope complete with field emission gun and sector field spectrometer coupled to a parallel recording system based on a silicon intensified target detector. The experimental energy resolution in this work was 0.5 eV; the collection and convergence semi-angles were 5 mrad and 4.3 mrad, respectively. This corresponds to a momentum transfer of 0.47 au^{-1}, which is well within the limit for the validity of the dipole approximation which in this case is of the order of 8 au^{-1}. Absolute energies were determined to within ± 0.2 eV. Spectra were taken from single-crystal specimens, scanning a sample area of about 600 Å on a side during data acquisition. No indication of specimen damage was observed. Specimen thicknesses were such that deconvolution to remove the effects of multiple scattering was deemed to be unnecessary for the comparison of near-edge

features. All samples were characterized prior to EELS analysis using a combination of x-ray and electron diffraction.

2.3. Theory

Theoretical modelling of near-edge features was performed using the ICXANES computer code of Vvedensky *et al* [10]. For all multiple-scattering calculations, phase shifts and matrix elements were obtained by imposing a muffin-tin potential on the structure in question [11]. Muffin-tin radii were chosen so as to minimize the discontinuity at touching muffin-tin spheres. Phase shifts up to $l = 3$ were employed and generally the cluster radius was chosen to be at least 10 au. The magnitude of the damping term was adjusted to give the best agreement with experiment; in all cases it was greater than the experimental energy resolution. Core hole effects were included by use of the $(Z + 1)^*$ approximation [12] for the central atom; however, the results were very similar to those obtained from using ground-state wavefunctions. Such an observation tends to support the argument of de Groot *et al* [6] that core hole effects should be small at the O K edges of transition-metal oxides.

3. Results and discussion

Figures 1 and 2 show the measured oxygen K ELNES of the various Ti(IV)–oxygen compounds together with the results of multiple-scattering calculations. In all spectra the energy scale is referred to the energy of the leading peak A, which has been set to zero. Absolute energies of the peaks A are given in table 1. Figure 3 shows the O K ELNES of the mineral titanite which we discuss at the end of this section. For all spectra, the background has been removed and the intensity normalized in an energy window extending 20 eV above the edge onset.

Table 1. Energies of the various features present in the O K ELNES of the titanium(IV)–oxygen compounds relative to the first strong peak A. The absolute energies of peaks A are given.

	Energy, region 1 (eV)			Energy, region 2 (eV)			
Compound	Edge onset	A	B	Minimum	C	D	E
Rutile TiO_2	−1.8	531.1	2.75	5.5	8.9	12.0	14.8
Anatase TiO_2	−1.4	530.9	2.60	5.1	7.9	11.2	13.8
Brookite TiO_2	−1.9	531.2	2.65	5.2	8.5	12.7	15.2
$FeTiO_3$	−1.7	531.4	2.55	4.4	7.1	10.6	13.6
$SrTiO_3$	−1.7	531.0	2.9				
$BaTiO_3$	−1.7	530.6	2.5				

A common characteristic feature of the spectra in figure 1 is the presence of two strong peaks, labelled A and B, in an energy range extending 7 eV above the edge onset (region 1). A deep minimum separates this first region from a second region which lies typically 7–20 eV above the edge threshold (region 2).

A characteristic feature of the spectra of the two perovskites, shown in figure 2, is that only one strong peak, peak A, is immediately apparent in region 1. The second peak, peak B, is visible but is strongly reduced in intensity. Moreover, these

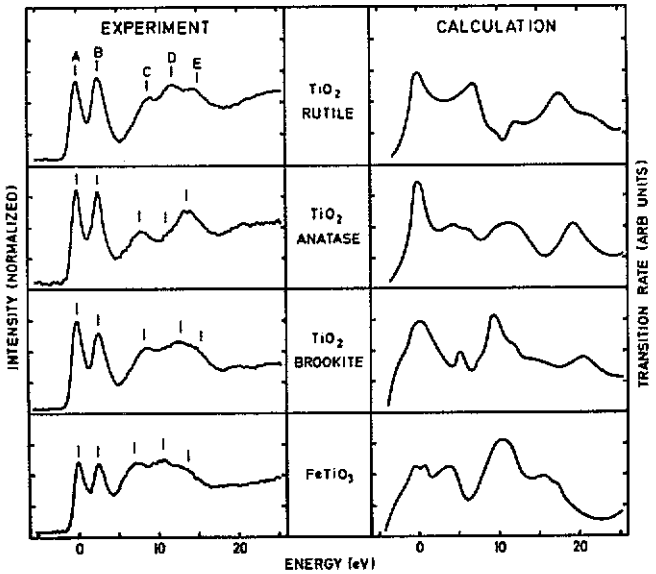

Figure 1. Oxygen K ELNES of the TiO_2 polymorphs rutile, anatase and brookite and of the mineral ilmenite $FeTiO_3$ together with the results of multiple-scattering calculations.

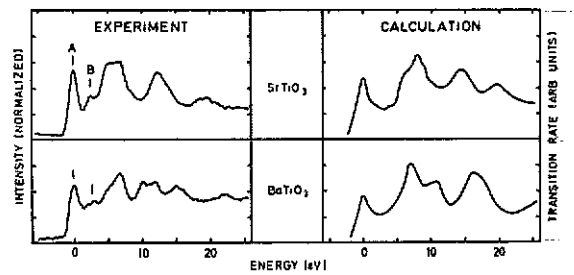

Figure 2. Oxygen K ELNES of the perovskites $SrTiO_3$ and $BaTiO_3$ together with the results of multiple-scattering calculations.

spectra do not clearly exhibit two separate regions because a higher-energy structure is superimposed on region 1.

The theoretical spectra shown in figures 1 and 2 have been aligned to experiment in such a way that the first peaks coincide. This is necessary owing to the arbitrary position of the muffin-tin energy zero. A general problem which has been observed before [5, 13] is that the theoretical energy scale does not agree with the experimental scale. The former is somewhat expanded, possibly owing to the theoretical approach which neglects the energy dependence of the exchange and correlation interactions between the excited electron and the predominantly O 2p valence electrons [14].

Considering the individual curves, the agreement between experiment and theory is good for the cubic perovskites which possess relatively high symmetry; the ICXANES calculations predicting the observed differences between $SrTiO_3$ and $BaTiO_3$. For the polymorphs of TiO_2 we have already published our ICXANES calculations of the O K edges in rutile and anatase [5], and we now add the results of our calculations for brookite. Here the agreement is not very satisfactory, especially in the case

of brookite; however, the general gross structure of the O K edge seems to be reproduced. Similar problems are also observed in the case of the $FeTiO_3$ ICXANES calculation and seem to be associated with the decrease in cluster symmetry employed in the multiple-scattering calculation.

The identification of the origin of the features observed in the experimental spectra may be achieved by progressively increasing the cluster size used in the multiple-scattering calculations [13]. We have found that the basic structure observed in region 1 is reproduced by using solely the first coordination shell of titanium (and iron in the case of $FeTiO_3$) atoms; the second coordination sphere which is composed of oxygen atoms (and Ba or Sr in the case of the perovskites) only reinforces this initial structure. The further structure in region 2 appears only after we add the oxygen and second metal coordination spheres and in order to produce all the observed structure we have to continue adding further shells. In terms of the scattering amplitudes of the various atomic types, the dominant scattering events in region 1 are d-like scattering from Ti and p-like scattering from O. In the case of the perovskites there also exists a contribution from s- and p-like scattering from Ba or Sr. As the energy increases and we enter region 2, the contribution of s- and p-like scattering from Ti is enhanced, in addition to d-like scattering from Ba or Sr in the perovskites.

For the case of the dioxide polymorphs and $FeTiO_3$, these results appear to be consistent with earlier findings [15]. In accordance with more recent work [6], region 1 essentially involves transitions to the narrow metal 3d band which is highly localized around the metal sites hybridized with oxygen 2p states; thus this region is essentially reproduced using the first coordination shell. Region 2 involves transitions to oxygen np states (predominantly $n = 2$ according to [6] and [16]) hybridized with the more delocalized transition-metal 4s and 4p states; thus we require further metal coordination shells to reproduce this structure.

Considering the titanium perovskites, band-structure calculations have predicted that the lower part of the conduction band (region 1) involves O 2p states hybridized with predominantly titanium 3d states [17–19]. This is confirmed by the results of our multiple-scattering calculations. Furthermore, the initial structure in our measured O K edge spectrum of $BaTiO_3$ shows a good agreement with the p-like DOS of $BaTiO_3$ computed by Balzarotti [20] from the results of Wolfram and Ellialtioglu [18] (who ignored the contribution of barium). Band-structure calculations have been performed for $SrTiO_3$ [19, 21] although none give the symmetry- and site-projected DOS which is necessary for comparison with experimental results. Turning to region 2, the band-structure calculation of Mattheiss [19] for $SrTiO_3$ predicts that this higher part of the conduction band involves O p states hybridized with transition-metal 4s and 4p states as well as 4d states of Sr (for $BaTiO_3$ this corresponds to the 5d states of Ba). This is again confirmed by our multiple-scattering calculations. However, Mattheiss [19] stresses that in $SrTiO_3$ the Sr 4d band overlaps with the top of region 1. This would then explain why the division of the perovskite spectra into two regions is less obvious than in the case of the dioxide polymorphs and $FeTiO_3$. We intend to clarify this point in a forthcoming publication.

We now discuss the structure in region 1 in more detail. First, we would like to emphasize that this effectively reflects the interactions of oxygen 2p orbitals with the titanium (transition-metal) 3d orbitals. As mentioned in [6] and [16], a purely ionic bond would block a dipole transition from the oxygen 1s level so that the presence of this structure gives some measure of the covalent character in the bonding which is known to be quite considerable in the case of transition-metal oxides.

In all the compounds considered, titanium is octahedrally coordinated to oxygen, the degree of distortion from a perfect octahedron varying amongst the oxides studied. A perfect octahedral ligand field causes the five degenerate d states in the conduction band to split into the twofold e_g states, the d_{z^2} and $d_{x^2-y^2}$ orbitals which are directed at the ligands, and the threefold t_{2g}, the d_{xy}, d_{yz} and d_{xz} orbitals which are directed between the ligands. The presence of distortions from octahedral symmetry causes further splitting, which is generally weaker than that produced by the main octahedral field, so that it is often still possible to identify t_{2g}-like and e_g-like orbitals. Thus in terms of the oxygen K edge we can identify two main types of interaction: the hybridization of oxygen 2p orbitals with t_{2g}-like Ti d orbitals which will be governed by pdπ interactions. Secondly, the hybridization of oxygen 2p orbitals with e_g-like Ti d orbitals which will be governed by pdσ interactions. Considering just the conduction band, since the overlap of the O 2p orbitals is greater with the e_g orbitals the σ^* (pdσ antibonding) band will be somewhat higher in energy than the π^* (pdπ antibonding) band. Looking at the spectra in figure 1, it is clear that we observe these π^* (t_{2g}-like) and σ^* (e_g-like) peaks (peaks A and B) in rutile, brookite, anatase and $FeTiO_3$. For these four samples, the splittings between these two peaks are all approximately equal to 2.6 eV which is roughly the same as is observed between the t_{2g}- and e_g-like bands on the corresponding titanium $L_{2,3}$-edge spectra [22] and these may be related to the ligand-field splittings of hydrated transition-metal ions in optical spectra [6, 23]. In the cubic perovskites (figure 2) the π^*–σ^* peak splitting is approximately the same as in the dioxides and $FeTiO_3$. However, the σ^* peak is much weaker and superimposed on a higher-energy structure. Thus the main feature in region 1 is the strong π^* peak and we believe this to be a fingerprint for oxygen in twofold linear coordination to titanium (transition metal) as we discuss below.

The results of the band-structure calculation of Munnix and Schmeits [24] on rutile is particularly informative because the site- and symmetry-resolved DOS are presented. Their partial DOS for the oxygen site shows a non-negligible contribution to the total DOS in the conduction band (which is primarily of Ti 3d character). They also show the O partial DOS decomposed into the contributions from oxygen p_x, p_y and p_z orbitals. If we choose the coordinate system so that the oxygen p_x and p_z orbitals lie in the Ti–O–Ti plane, then it is clear that both p_x and p_z orbitals undergo pdσ and pdπ interactions with Ti d orbitals, while p_y orbitals can only interact through pdπ interactions. The resultant oxygen partial DOS shows two main peaks of equal height separated by about 2.5 eV in agreement with our measured O K edge spectrum of rutile. Applying this coordinate system to the oxygen site geometry encountered in the cubic perovskites and choosing the x direction to lie along the Ti–O–Ti direction simplifies the discussion. The p_x orbital then undergoes solely pdσ interactions while, for the p_y and p_z orbitals, only pdπ interactions are non-zero. Qualitatively it is easy to see that pdσ interactions will be drastically reduced and pdπ interactions somewhat increased in linear twofold coordination compared with the threefold coordination of titanium to oxygen in rutile. This would then explain the diminution in the σ^* peak in the O K ELNES of the cubic perovskites which is also predicted by our ICXANES calculations. In the case of anatase TiO_2, we have, as in rutile, threefold planar coordination of titanium to oxygen and the relative intensities of the π^* and σ^* peaks are very similar to those in rutile. The oxygen coordination in brookite TiO_2 is again threefold but all atoms do not lie in a single plane, although the distortion is small. However, simplistically we would expect this to affect predominantly the pdσ interactions of the p_x and p_z orbitals, causing these to diminish relative to those in

the planar case (the pdσ interactions are more sensitive to distortions than are the pdπ interactions [25]). This would then result in a decrease in the intensity in the σ^* peak relative to the π^* peak in brookite compared with those found in rutile and anatase, which is in agreement with experiment (figure 1).

For the case of regular tetrahedral coordination, and therefore also the distorted tetrahedral coordination of oxygen present in $FeTiO_3$, all the three oxygen 2p orbitals would undergo both pdπ and pdσ interactions and again we observe two strong peaks of similar intensities in region 1. However, the presence of two differing 3d transition metal ions, Ti^{4+} (d^0) and Fe^{2+} (d^6) in the first coordination sphere further complicates matters. The relative intensities of the π^* and σ^* peaks depend on the number of d electrons present in the t_{2g}-like and e_g-like bands, although it has been shown [6] that this relationship is not simple. Ti_2O_3 contains Ti^{3+} ions (d^1) in a corundum structure [7] and the coordination of titanium to oxygen is similar to that in $FeTiO_3$. The O K edge spectrum of this compound also shows two strong peaks of similar intensities in region 1 [6]. TiO contains Ti^{2+} ions (d^2) in a rocksalt structure [7]; here six titanium atoms are octahedrally coordinated to oxygen. The O K edge spectrum of this compound also exhibits two strong peaks of similar intensities in region 1 [26]. Again all three oxygen 2p orbitals would interact with the Ti 3d orbitals through pdπ and pdσ interactions. The O K ELNES of both TiO and Ti_2O_3 has been successfully modelled using ICXANES calculations [27].

Turning to region 2, we can make the following general points. As discussed above, our multiple-scattering studies indicate that this arises from the outer-lying shells of atoms, the heavier metal ions being important contributors to the scattering. Considering the cubic perovskites, the high-symmetry results in well ordered and well separated shells surrounding the central oxygen atom and this produces a considerable fine structure compared with the lower symmetry of the dioxides and ilmenite. Furthermore, substituting the stronger-scattering barium for strontium in the perovskite structure causes the experimental ELNES in this region to become considerably more complex (figure 2). Amongst the titanium dioxides it is clear that rutile and anatase exhibit a more well defined structure in region 2 than does brookite which has two differing oxygen sites of lower symmetry. De Groot *et al* [6] have demonstrated the decrease in intensity of region 1, the 3d band, relative to region 2, the 4sp band, for 3d transition-metal oxides which primarily arises from the decrease in the number of d states available for hybridization with O 2p levels. This may be seen in our data by comparing the relative intensities of regions 1 and 2 for the dioxides and for $FeTiO_3$ (figure 1).

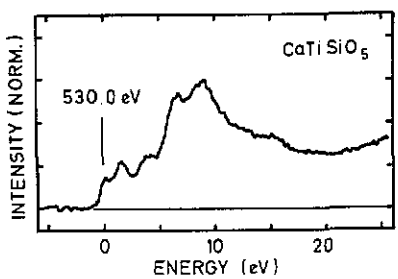

Figure 3. Oxygen K ELNES of the mineral titanite ($CaTiSiO_5$) which contains three chemically and structurally inequivalent oxygen sites.

Finally, in figure 3, we consider the oxygen K edge spectrum of the mineral titanite. It shows a very complicated structure which, in our experience, is very unusual for such an edge. The presence of oxygen in differing chemical environments would be expected to lead to different 'effective charges' on the atoms in question, which in turn should lead to differing core level binding energies. Using Pauling's method to calculate the net charges on the oxygen atoms arising from the different nearest neighbours together with a charge potential model, we have previously shown [4] that it is possible to calculate the potential energy experienced by an oxygen 1s core electron on each of the differing sites. Such a calculation on the oxygen sites in titanite results in the fact that the O(2) and O(1) sites are at very similar effective core potentials; their relative occupancies are 2 and 1, respectively. Concentrating initially on just the metal nearest neighbours, the O(3) site with relative occupancy 2 lies at a much lower potential than the other two sites. This potential is about 10 eV more negative and increases with the inclusion of the effect of neighbouring oxygen atoms in our calculation. Since we do not know the precise form of the edge for each site it is difficult to perform a fit to the experimental data as we have done before [4]. However, from our previous analyses of the oxygen sites in the minerals rhodizite [4] and wollastonite [27], we confirmed the expected linear dependence of the binding energy with calculated effective core potentials and obtained a gradient k of about 0.5. Using this value, we derive a value of at least 5 eV for the binding energy separation between the O(3) and the O(2) plus O(1) sites. The absolute value is dependent on whether or not we include the effect of the close approach of the oxygen on the O(3) site. This procedure assumes that we may use the k-value derived from the minerals rhodizite and wollastonite in the analysis of titanite. If we assign the peak at about 530 eV to the onset of the structure due to the O(3) site, the O(2) and O(1) sites would then begin to contribute at least 5 eV above this, which corresponds to the steep rise in the observed edge. On consideration, the general shape of the edge for each oxygen site probably involves a weaker low-energy structure corresponding to transitions to oxygen 2p states hybridized with transition-metal 3d levels (presumably derived from the Ti neighbours), together with a more intense structure at higher energy loss corresponding to transitions to oxygen p states hybridized with s and p states of the various nearest neighbours. The superposition of such structures in the ratio 2:3 separated by about 5 eV or more could convincingly lead to the observed edge features.

4. Conclusions

Modelling of spectra by multiple-scattering calculations allows a detailed interpretation of the measured O K ELNES of titanium(IV)–oxygen compounds. This has been achieved by progressively increasing the size of the cluster used in the calculation. The spectra may be essentially divided into two regions. Region 1, up to 7 eV above the edge onset, corresponds to transitions to final states consisting of oxygen 2p character hybridized with transition-metal 3d character. Region 2, ranging from 7 to 20 eV above the threshold, corresponds to transitions to final states of mixed oxygen 2p–transition-metal 4s and 4p character. In the case of the perovskites this region 2 also contains alkaline-earth d character. A detailed discussion of the structure in region 1 with reference to the number and geometry of the titanium nearest neighbours suggests that the observed O K ELNES of the perovskites is characteristic of oxygen

in linear twofold coordination and may be used as a fingerprint. We also qualitatively account for the complex spectrum obtained from titanite in terms of differing oxygen site occupancies.

Acknowledgments

We would like to acknowledge financial support from the Royal Society (for a Pickering Research Fellowship to RB) and the continued interest of Professor E Zeitler.

References

[1] Colliex C, Manoubi T, Gasgnier M and Brown L M 1985 *Scanning Electron Microsc.* **2** 489
[2] Hofer F and Golob P 1987 *Ultramicroscopy* **21** 379
[3] Williams B G 1987 *Prog. Solid State Chem.* **17** 87
[4] Brydson R, Williams B G, Sauer H, Engel W, Schlogl R, Muhler M, Zeitler E and Thomas J M 1988 *J. Chem. Soc. Faraday Trans.* I **84** 631
[5] Brydson R, Sauer H, Engel W, Thomas J M, Zeitler E, Kosugi N and Kuroda H 1989 *J. Phys.: Condens. Matter* **1** 797
[6] de Groot F M F, Grioni M, Fuggle J C, Ghijsen J, Sawatzky G A and Petersen H 1989 *Phys. Rev.* B **40** 5715
[7] Wyckoff R W G 1960 *Crystal Structures* (New York: Interscience)
[8] $BaTiO_3$ is tetragonal below 120 °C; however, this distortion does not affect our arguments.
[9] Engel W, Sauer H, Brydson R, Williams B G, Zeitler E and Thomas J M 1988 *J. Chem. Soc. Faraday Trans.* I **84** 617
[10] Vvedensky D D, Saldin D K and Pendry J B 1986 *Comput. Phys. Commun.* **40** 421
[11] Mattheiss L F 1964 *Phys. Rev.* A **133** 1399
Loucks T L 1967 *Augmented Plane Wave Method* (New York: Benjamin)
[12] Brydson R, Vvedensky D D, Engel W, Sauer H, Williams B G, Zeitler E and Thomas J M 1988 *J. Phys. Chem.* **92** 962
Brydson R, Bruley J and Thomas J M 1988 *Chem. Phys. Lett.* **149** 343
[13] Lindner Th, Sauer H, Engel W and Kambe K 1986 *Phys. Rev.* B **33** 22
[14] Davoli I, Marcelli A, Bianconi A, Tomellini M and Fanfoni M 1986 *Phys. Rev.* B **33** 2979
[15] Grunes L A, Leapman R D, Wilker C N, Hoffman R and Kunz A B 1982 *Phys. Rev.* B **25** 7157, and references therein
[16] Pedio M, Fuggle J C, Somers J, Umbach E, Haase J, Lindner Th, Hofer U, Grioni M, de Groot F M F, Hillert B, Becker L and Robinson A 1989 *Phys. Rev.* B **40** 7924
[17] Pertosa P and Michel-Calendini F M 1978 *Phys. Rev.* B **17** 2011
[18] Wolfram T and Ellialtioglu 1982 *Phys. Rev.* B **25** 2697
[19] Mattheiss L F 1972 *Phys. Rev.* B **6** 4718
[20] Balzarotti A 1983 *EXAFS and Near-edge Structures* ed A Bianconi, L Incoccia and S Stipcich (Berlin: Springer) p 135
[21] Soules T F, Kelly E J, Vaught D M and Richardson J W 1972 *Phys. Rev.* B **6** 1519
[22] Engel W and Sauer H 1990 *Proc. 12th Int. Congr. on Electron Microscopy* vol 2 (San Francisco: San Francisco Press) p 70
[23] Brydson R, Williams B G, Engel W, Sauer H, Zeitler E and Thomas J M 1987 *Solid State Commun.* **64** 609
[24] Munnix S and Schmeits M 1984 *Phys. Rev.* B **30** 2202
[25] Ballhausen C J 1962 *Introduction to Ligand Field Theory* (New York: McGraw-Hill)
[26] Nakai S, Mitsuishi T, Sugawara H, Maezawa H, Matsukawa T, Mitani S, Yamasaki K and Fujikawa T 1987 *Phys. Rev.* B **36** 9241
[27] Brydson R 1988 *PhD Thesis* University of Cambridge